DOC. NO._____

COPY NO._____

HEADQUARTERS
OFFICE OF THE DEPUTY COMMANDER AFSC
FOR AEROSPACE SYSTEMS
UNITED STATES AIR FORCE

Flow of Gas-Particle Mixtures in Axially Symmetric Nozzles

by
James R. Kliegel
and
Gary R. Nickerson

FLOW OF GAS-PARTICLE MIXTURES IN AXIALLY SYMMETRIC NOZZLES

by - James R. Kliegel
and
Gary R. Nickerson

SPACE TECHNOLOGY LABORATORIES, INC.
P. O. Box 95001
Los Angeles 45, California

1713-61

ABSTRACT

A previous study (1) of one-dimensional gas-particle nozzle flows has been expanded to treat axially symmetric nozzle flows. Comparisons between calculated and experimentally measured nozzle efficiencies are given for a metallized double base propellant whose exhaust contains 38% condensed oxides. It is shown that the theory predicts the performance of this propellant in nozzles of greatly different size, shape and expansion ratio, within the limits of the experimental measurements. It is concluded that the theory adequately describes the flow of gas-particle mixtures in axially symmetric nozzles.

NOMENCLATURE

C_D	-	Particle drag coefficient
C_{pg}	-	Gas heat capacity
C_{pl}	-	Particle heat capacity ($T_p > T_{pm}$)
C_{ps}	-	Particle heat capacity ($T_p < T_{pm}$)
f_p	-	Ratio, $C_D/(C_D)_{Stokes}$
g_p	-	Ratio, $Nu/(Nu)_{Stokes}$
h	-	Film heat transfer coefficient
h_p	-	Particle enthalpy
h_{pl}	-	Particle enthalpy after melting ($T_p = T_{pm}$)
h_{ps}	-	Particle enthalpy before melting ($T_p = T_{pm}$)
k_g	-	Gas thermal conductivity
L	-	Nozzle length
	-	Gas Mach number
m_p	-	Particle density
Nu	-	Particle Nusselt number, $2hr_p/k_g$
P_g	-	Gas pressure
Pr	-	Gas Prandtl number $\mu_g C_{pg}/k_g$
R	-	Gas constant
R^*	-	Nozzle wall radius of curvature at nozzle throat
r	-	Radial coordinate
r_p	-	Particle radius
r^*	-	Nozzle throat radius
T_g		Gas temperature

T_p - Particle temperature

T_{pm} - Particle solidification temperature

U_g - Gas axial velocity

U_p - Particle axial velocity

V_g - Gas radial velocity

V_p - Particle radial velocity

z - Coordinate in flow direction

γ_g - Gas adiabatic expansion coefficient

$\bar{\gamma}$ - Equilibrium expansion coefficient for gas-particle system

ϵ - Nozzle expansion ratio

θ - Conical nozzle cone angle

θ_e - Nozzle exit lip angle

θ_i - Nozzle inlet angle

θ_j - Nozzle initial expansion angle

μ_g - Gas viscosity coefficient

ρ_g - Gas density

ρ_p - Particle density in the gas (based on gas volume)

ψ_p - Particle stream function

Superscript

$*$ - Refers to throat conditions

I N T R O D U C T I O N

Experience has shown that the efficiency of metallized propellants (delivered impulse/theoretical impulse) is lower than the efficiency of non-metallized propellants. This decreased efficiency has been found to be approximately proportional to the particle weight fraction in the exhaust gases. In addition, performance losses have been observed when using optimum contoured nozzles (calculated assuming gas-particle equilibrium) with metallized propellants. These facts suggest that non-equilibrium gas-particle effects should be considered when making performance predictions for metallized propellants. A study (1) was first made of one dimensional gas-particle nozzle flows. It was found that gas-particle non-equilibrium effects become important if the particle diameter is greater than one micron. For larger particle sizes, the predicted non-equilibrium effects were in qualitative agreement with experimental results. The present investigation is essentially an extension of the above study to axially symmetric gas-particle nozzle flows.

CHARACTERISTIC RELATIONSHIPS OF GAS-PARTICLE SYSTEMS

The equations governing the flow of a gas-particle mixture have been previously derived (2) and are given below for axially symmetrical flows:

$$(\rho_g u_g)_z + \frac{1}{r}(r\rho_g v_g)_r = 0 \tag{1}$$

$$(\rho_p u_p)_z + \frac{1}{r}(r\rho_p v_p)_r = 0 \tag{2}$$

$$\rho_g\left[u_g(u_g)_z + v_g(u_g)_r\right] + \frac{9}{2}\frac{\mu_g \rho_p \ell_p}{m_p n_p^2}(u_g - u_p) + (P_g)_z = 0 \tag{3}$$

$$\rho_g\left[u_g(v_g)_z + v_g(v_g)_r\right] + \frac{9}{2}\frac{\mu_g \rho_p \ell_p}{m_p n_p^2}(v_g - v_p) + (P_g)_r = 0 \tag{4}$$

$$u_g(P_g)_z + v_g(P_g)_r - \gamma_g R T_g\left[u_g(\rho_g)_z + v_g(\rho_g)_r\right]$$

$$+ \frac{9}{2}\frac{\mu_g \rho_p \ell_p}{m_p n_p^2}(\gamma_g - 1)\left[(u_g - u_p)^2 + (v_g - v_p)^2 + \frac{2}{3}\frac{q_p}{\ell_p}\frac{C_{pg}}{P_r}(T_p - T_g)\right] = 0 \tag{5}$$

$$P_g = \rho_g R T_g \tag{6}$$

$$u_p(u_p)_z + v_p(u_p)_r = \frac{9}{2}\frac{\mu_g \ell_p}{m_p n_p^2}(u_g - u_p) \tag{7}$$

$$u_p(v_p)_z + v_p(v_p)_r = \frac{9}{2}\frac{\mu_g \ell_p}{m_p n_p^2}(v_g - v_p) \tag{8}$$

$$u_p(\ell_p)_z + v_p(\ell_p)_r = -3\frac{\mu_g q_p}{m_p n_p^2}\frac{C_{pg}}{P_r}(T_p - T_g) \tag{9}$$

where

$$T_p = T_{pm} + \frac{\ell_p - \ell_{pe}}{C_{pe}}, \quad \ell_p \geq \ell_{pe} \tag{10a}$$

$$T_p = T_{p_{max}} \quad , \quad h_{p_1} \geq h_p > h_{p_2} \tag{10b}$$

$$T_p = \frac{h_p}{C_{p_2}} \quad , \quad h_{p_2} \geq h_p \tag{10c}$$

(For simplicity of presentation, only one particle size will be considered in the derivation of the characteristic relationships of gas-particle systems in this report. Complete details of the theoretical treatment of gas-particle flows (including consideration of a particle size distribution in the flow) are given in reference (2). The calculations presented in this paper consider the measured particle size distribution (3) present in the flow unless otherwise noted.)

The basic assumptions made in deriving the above equations are:

(1) There are no mass or energy losses from the system.

(2) The particles do not interact.

(3) The thermal (Brownian) motion of the particles does not contribute to the pressure of the system.

(4) The internal temperature of the particles is uniform.

(5) Energy exchange occurs between the particles and the gas only by convection.

(6) The gas is considered to be a perfect gas of constant composition.

(7) The gas is inviscid except for the drag it exerts on the particles.

(8) The thermal heat capacities of the gas and particles are constant.

(9) The volume occupied by the particles is negligible.

These same assumptions have been used in previous studies (1, 4) of the one dimensional flow of gas-particle systems.

It has been found (2) that the complete system of characteristics of the above equations are:

Along gas streamlines

$$\frac{dr}{dz} = \frac{v_g}{u_g} \tag{11}$$

$$\rho_g\left[u_g du_g + v_g dv_g\right] + dP_g = -\frac{9}{2}\frac{\mu_g \rho_p \ell_p}{m_p n_p^2}\left[(u_g-u_p)dz + (v_g-v_p)dr\right] \tag{12}$$

$$\frac{dP_g}{P_g} - \gamma_g\frac{d\rho_g}{\rho_g} = -\frac{9}{2}\frac{\mu_g \rho_p \ell_p}{m_p n_p^2}\frac{(\gamma_g-1)}{\rho_g u_g}\left[(u_g-u_p)^2 + (v_g-v_p)^2 + \frac{2}{3}\frac{q_p}{\ell_p}\frac{C_{pa}}{P_a}(T_p-T_g)\right]dz \tag{13}$$

Along gas Mach lines

$$\frac{dr}{dz} = \frac{u_g v_g \pm \gamma_g R T_g\sqrt{M^2-1}}{u_g^2 - \gamma_g R T_g} \tag{14}$$

$$(u_g\frac{dr}{dz} - v_g)\left\{\frac{9}{2}\frac{\mu_g \rho_p \ell_p}{m_p n_p^2}(\gamma_g-1)\left[(u_g-u_p)^2 + (v_g-v_p)^2 + \frac{2}{3}\frac{q_p}{\ell_p}\frac{C_{pa}}{\mu}(T_p-T_g)\right]dz\right.$$

$$-u_g dP_g \Big] + \gamma_g R T_g \left\{ \frac{9}{2} \frac{\mu_g \rho_p \ell_p}{m_p r_p^2} \left[(u_g - u_p) dr - (v_g - v_p) dz \right] + \rho_g \left[v_g du_g \right.\right.$$

$$\left.\left. - u_g dv_g - \frac{v_g}{r} (u_g dr - v_g dz) \right] + dP_g \frac{dr}{dz} \right\} = 0 \qquad (15)$$

Along particle streamlines,

$$\frac{dr}{dz} = \frac{v_p}{u_p} \qquad (16)$$

$$u_p du_p = \frac{9}{2} \frac{\mu_g \ell_p}{m_p r_p^2} (u_g - u_p) dz \qquad (17)$$

$$v_p dv_p = \frac{9}{2} \frac{\mu_g \ell_p}{m_p r_p^2} (v_g - v_p) dr \qquad (18)$$

$$u_p dh_p = -3 \frac{\mu_g q_p}{m_p r_p^2} \frac{C_{pg}}{P_r} (T_p - T_g) dz \qquad (19)$$

$$d\psi_p = 0 \qquad (20)$$

where ψ_p is the particle stream function defined by

$$(\psi_p)_r = r \rho_p u_p \qquad (20a)$$

$$(\psi_p)_z = -r \rho_p v_p \qquad (20b)$$

It is seen that all the characteristics of the equations governing the flow of a gas-particle system are real if the flow is supersonic ($M > 1$). Using the above relationships, one may

compute the supersonic flow of a gas-particle mixture using the method of characteristics. Figure I illustrates the characteristic mesh.

It is interesting to note that one of the characteristic directions of the above equations is identical with the gas Mach lines independent of the presence of the particles. This result is similar to the situation found in reacting gas mixtures (5) in which one of the characteristic directions is also identical with the gas Mach lines independent of chemical reactions occurring in the flow.

TRANSONIC FLOW OF A GAS-PARTICLE SYSTEM

To solve the equations governing the transonic flow of a gas-particle mixture is an extremely formidable task. For perfect gas flows, one can obtain approximate transonic solutions by taking perturbations about the sonic velocity (6, 7). This method is applicable for perfect gas flows because the throat conditions are essentially determined by the nozzle geometry in the immediate neighborhood of the throat and are quite insensitive to the nozzle inlet geometry. This is not true for gas-particle flows as the throat conditions are determined by the nozzle inlet geometry (1). Thus to obtain initial conditions to start a characteristic calculation for a gas-particle system, one must solve for the complete

subsonic and transonic flow field in the nozzle inlet and throat regions.

One can obtain interesting qualitative information about the transonic flow of a gas-particle mixture by such a perturbation method however. Let us consider a gas-particle nozzle flow which is essentially in equilibrium. The gas properties in the transonic throat region can be approximated by (1, 6)

$$\frac{u_g}{u_g^*} = 1 + \alpha \frac{z}{n^*} + \frac{\bar{\gamma}+1}{8} \alpha^2 \frac{n^2}{n^{*2}} \tag{21}$$

$$\frac{v_g}{u_g^*} = \frac{\bar{\gamma}+1}{4} \alpha^2 \frac{zn}{n^{*2}} + \frac{(\bar{\gamma}+1)^2}{16} \alpha^3 \frac{n^3}{n^{*3}} \tag{22}$$

where

$$\alpha = \sqrt{\frac{2}{\bar{\gamma}+1} \frac{n^*}{R^*}} \tag{23}$$

and the nozzle throat location is given by

$$\frac{z^*}{n^*} = -\sqrt{\frac{\bar{\gamma}+1}{32} \frac{n^*}{R^*}} \tag{24}$$

From equations (7) and (8) we find that to Sauer's order of approximation

$$\frac{u_p}{u_g^*} = K\left(1 + \alpha \frac{z}{n^*} + \frac{\bar{\gamma}+1}{8} \alpha^2 \frac{n^2}{n^{*2}}\right) \tag{25}$$

$$\frac{v_p}{u_g^*} = K\left[\frac{\bar{\gamma}+1}{4}\alpha^2\left(\frac{2}{n^*} - \frac{2}{9}\frac{m_p n_p^2}{\mu_g^* \rho_{bp}^*}\frac{u_g^*}{n^*}\right)\frac{n}{n^*} + \frac{(\bar{\gamma}+1)^2}{16}\alpha^3\frac{n^3}{n^{*3}}\right] \tag{26}$$

where

$$K = 1 - \frac{2}{9}\frac{m_p n_p^2}{\mu_g^* \rho_{bp}^*}\frac{u_g^*}{n^*}\alpha \;, \qquad \frac{2}{9}\frac{m_p n_p^2}{\mu_g^* \rho_{bp}^*}\frac{u_g^*}{n^*} \ll 1 \tag{27}$$

Examination of the above equations show that the particle and gas streamlines diverge in the throat region for all particle sizes even though the flow may be essentially in equilibrium. Thus the particles concentrate along the nozzle axis which greatly complicates calculation of the gas-particle flow properties in the nozzle throat. This is illustrated in Figure II.

It has been shown (1) that the Mach number in a gas-particle nozzle flow is less than one at the nozzle throat. For typical metallized propellants calculations show that the Mach number is approximately .8 at the throat. Hence, the transonic zone in a gas-particle flow extends downstream of the throat. Because of this, a discontinuity in the wall radius of curvature at the throat will have a great influence on the flow. Thus it will be extremely difficult to calculate the gas-particle flow properties in a throat region of a nozzle having different wall radii of curvatures upstream and downstream of the throat.

From the above discussion, it is evident that one can only obtain approximate solutions to the equations governing the transonic flow of a gas-particle system. In order to reduce the complexity of the calculations, the nozzle inlet and throat geometry considered in this study consisted of a conical inlet section joined smoothly to a constant radius of curvature throat section. This geometry is shown in Figure III. It is believed that this simplified geometry adequately represents the inlet and throat geometry of nozzle configurations of interest.

APPROXIMATE METHOD FOR OBTAINING GAS-PARTICLE TRANSONIC FLOW CONDITIONS

The following method was used to obtain approximate initial conditions for the characteristic calculations. In the conical inlet section, the flow was assumed to be a one-dimensional sink flow. The equations governing the one-dimensional flow of a gas-particle system were solved to obtain the flow properties on the sink line. The gas properties in the throat region were approximated by the perfect gas relationships and particle trajectories were calculated through the throat region to determine the particle properties along the initial line. An average expansion coefficient approximating the gas-particle expansion (including the effects of gas-particle non-equilibrium) was used (1).

The initial conditions thus determined were self-consistent as the characteristic calculations proceeded smoothly away from the initial line. Comparisbn of the nozzle weight flows obtained by the above method with those obtained by one-dimensional calculations shows that the two-dimensional weight flows are slightly less than the one-dimensional weight flows. This agrees with the results obtained (8) i . perfect gases. In addition, the above method of obtaining the gas-particle flow properties along the initial line is exact for the case of gas-particle equilibrium. It is concluded that the gas-particle flow properties determined along the initial line by the above method are an adequate representation of the true flow properties for nozzle calculations.

COMPARISON OF EXPERIMENTAL NOZZLE FIRINGS WITH CALCULATED NOZZLE PERFORMANCE

The experimental nozzle firings which will be compared with the calculations are firings conducted by the Hercules Powder Company. The altitude nozzle firings were conducted at the Arnold Engineering Development Center and the sea level nozzle firings were conducted at the Hercules facility in Baccus, Utah. Similar firings were made at both facilities which allows direct comparison of firings at either site. Most of the altitude nozzle firings have been previously reported (9).

All of the firings were of short duration and were made with engines containing a metallized double base propellant whose combustion products contain 38% condensed metal oxides. Most of the firings were made with forty pound charge (FPC) engines whose configuration is shown in Figure IV. Various nozzle configurations were tested and the parameters used to identify the nozzles are shown in Figure V.

All comparisons of experimental and calculated nozzle performances will be made on the basis of engine efficiency (delivered or calculated impulse/theoretical impulse). It has been assumed that the calculated theoretical impulse is correct and no allowance has been made for possible inaccuracies in this calculation.

In order to separate expansion losses from engine heat losses and nozzle friction, these quantities have been calculated following the method suggested by Bartz (10). The calculated heat and friction losses as well as the experimentally measured engine efficiencies are given in Table I for a series of conical nozzles. The difference between the calculated heat and friction losses and the measured engine losses was assumed to be expansion loss due to gas-particle non-equilibrium in the nozzle.

Calculations of the expansion losses in these nozzles due to gas particle non-equilibrium in the nozzles are given in Table II. These calculations were made assuming various particle size distributions present in the flow. The particle size distributions considered were

the nominal particle size distribution measured during these firings (3) and possible particle size distributions (1σ light and 1σ heavy) within the accuracy of the measurements.

It is seen that within the accuracy with which the various quantities are known, the calculated losses due to gas-particle non-equilibrium in the nozzle are in reasonable agreement with the experimental measurements if one assumes the 1σ light particle size distribution is present in the flow. Although the theory seems to over estimate the gas-particle non-equilibrium losses on the basis of nominal estimates of all quantities, it is felt that the agreement between the calculations and the experimental measurements is quite good especially when one considers that no allowance has been made for possible inaccuracies in the calculated theoretical impulses. In all further comparisons between the calculations and experimental measurements, it has been assumed that the 1σ light particle size distribution is present in the flow. In addition, the calculations have been adjusted slightly (less than .5% in all cases) to fit one of the experimental measurements in the set of nozzles being compared.

One of the more interesting predictions of the previous one-dimensional study (1) is that the throat conditions for a gas-particle exhaust flow are fixed by the nozzle inlet geometry and that one can change nozzle performance by changing only the nozzle inlet geometry. Table III compares the experimental and calculated performance of a set of cut-off

nozzles (ϵ = 1) in which only the wall radius of curvature in the throat section was varied. Table IV compares the experimental and calculated performance of a set of nozzles in which only the nozzle inlet angle was varied. It is seen that the predicted variation of performance with changes in nozzle inlet geometry is confirmed by experiment.

Table V compares the performance of similar nozzles of different throat size with the calculated scaling effects. (The TPC engine is essentially a 1/3 scale FPC and the Be-1 engine is similar to the ABL-X248 engine. Although these nozzles do not have identical inlets, calculations show that the performances of the TPC and Be-1 nozzles are identical with geometrically scaled FPC nozzles.) It is seen that the predicted scaling effects are confirmed by experiment.

Table VI and VII compare the experimental and calculated performance of conical and contoured nozzles of the same length and expansion ratio. It is seen that the calculations adequately predict the performance of the contoured nozzles. It is of interest to note that particle impingement occurred on the lips of the two contoured nozzles in Table VI. The calculations predicted particle impingement on the lip of the more highly contoured nozzle.

Table VII compares one-dimensional and the axially symmetric calculations for a set of conical nozzles. It is seen that the one-dimensional calculations underestimate the expansion losses due to gas-

particle non-equilibrium by approximately .75%. It thus appears that one can estimate gas-particle non-equilibrium losses quite adequately for conical nozzles through use of one-dimensional gas-particle calculations.

SUMMARY

From the above comparisons of experimental and calculated nozzle efficiencies of metallized propellants it is concluded that one can predict the efficiency of these propellants by considering engine heat and friction losses and expansion losses due to gas-particle non-equilibrium in the nozzle.

It has been shown that the theoretical predictions of the effects of the nozzle inlet and throat section, nozzle contouring and nozzles size on performance are in reasonable agreement with experiment. It is concluded that present theoretical treatment adequately describes axially symmetric gas-particle nozzle flows.

ACKNOWLEDGEMENTS

The authors would like to thank the Hercules Powder Company for allowing the use of their experimental nozzle firings as examples in this report. The work of Dr. Loren Morey, Dr. Billings Brown and Mr. Robert Barry in planning and conducting these nozzle tests is gratefully acknowledged.

REFERENCES

(1) Kliegel, J. R. 'One Dimensional Flow of a Gas-Particle System', presented at the 28th annual meeting of the IAS, New York, New York, January 1960. IAS Paper No. 60-S.

(2) Kliegel, J. R. and Nickerson, G. R. 'Calculation of Gas-Particle Flows in Axially Symmetric Nozzles', Space Technology Laboratories Report 7106-0017-RU-000, March 1961.

(3) Brown, B. 'Particle Size of Condensed Oxides from Combustion of Metalized Solid Propellants', presented at the 8th International Combustion Symposium, Pasadena, California, September 1960.

(4) Carrier, G. F. 'Shock Waves in a Dusty Gas', J. Fluid Mech. 4, 376 (1958).

(5) Vincenti, W. G. 'Non-equilibrium Flow Over a Wavy Wall', J. Fluid Mech. 6, 481 (1959).

(6) Sauer, R. 'General Characteristics of the Flow Through Nozzles at Near Critical Speeds', NACA TN 147 (1947).

(7) Kliegel, J. R. 'Higher Order Approximations to the Transonic Flow in a Nozzle Throat', Space Technology Laboratories Report 7106-0016-RU-000, March 1961.

(8) Emmons, K. W. 'The Theoretical Flow of a Frictionless, Adiabatic, Perfect Gas Inside of a Two-Dimensional Hyperbolic Nozzle', NACA TN 1003 (1946).

(9) Winer, R. and Morey, L. 'Nozzle Design for Solid Propellant Rockets', Presented at the Solid Propellant Rocket Research Conference, Princeton New Jersey, January 1960. ARS preprint 1046-60.

(10) Bartz, D. R. 'A Simple Equation for Rapid Estimation of Rocket Nozzle Convective Heat Transfer Coefficients', Jour. ARS, 27, 49 (1957).

TABLE I

Measured Gas-Particle Non-Equilibrium Expansion Losses in Conical Nozzles

ϵ	3.5	20	24	24	24	24
No. Firings	2	3	8	3	2	2
r^*	1.32"	1.32"	1.32"	1.32"	1.32"	1.32"
R^*/r^*	2	2	2	5	5	5
θ_i	30°	30°	30°	30°	30°	30°
θ	25.2°	21.5°	24°	12°	18°	24°
Calc. Heat Losses	$.6\pm.2\%$	$.8\pm.2\%$	$.9\pm.3\%$	$1.3\pm.4\%$	$1.1\pm.3\%$	$1.0\pm.3\%$
Calc. Friction Losses	$.7\pm.2\%$	$1.5\pm.5\%$	$1.4\pm.4\%$	$2.9\pm.9\%$	$2.0\pm.6\%$	$1.6\pm.5\%$
Meas. Engine Efficiency	$95.4\pm.3\%$	$94.7\pm.3\%$	$94.7\pm.6\%$	$95.1\pm.3\%$	$95.1\pm.3\%$	$95.1\pm.3\%$
Meas. Expansion Losses	$3.3\pm.7\%$	$3.0\pm1.0\%$	$3.0\pm1.3\%$	$.7\pm1.6\%$	$1.8\pm1.2\%$	$2.3\pm1.1\%$

TABLE II

Calculated Gas-Particle Non-Equilibrium Expansion Losses in Conical Nozzles

ϵ	3.5	20	24	24	24	24
No. Firings	2	3	12	3	2	2
r^*	1.32"	1.32"	1.32"	1.32"	1.32"	1.32"
R^*/r^*	2	2	2	5	5	5
θ_i	30°	30°	30°	30°	30°	30°
θ	25.2°	21.5°	24°	12°	18°	24°
Calc. Expansion Losses	$5.0\pm1.0\%$	$4.8\pm1.0\%$	$4.9\pm1.0\%$	$3.5\pm1.0\%$	$4.1\pm1.0\%$	$4.6\pm1.0\%$

TABLE III

Comparison of The Experimental and Calculated
Effect of Changes in The Nozzle Throat Geometry

ϵ	1	1	1	1	1	1	1
No. Firings	1	3	3	3	3	3	3
r^*	1.32"	1.45"	1.32"	1.32"	1.32"	1.32"	1.32"
R^*/r^*	1	2	3	5	7	9	15
θ_i	30°	30°	30°	30°	30°	30°	30°
Meas. Efficiency	91.5%	90.5±.4%	92.2±.4%	91.6±.3%	92.3±.5%	92.9±.3%	93.1±.5%
Calc. Efficiency	90.6%	91.3%	91.8%	92.3%	92.6%	92.9%	93.2%

TABLE IV

Comparison of The Experimental and Calculated
Effect of Changes in The Nozzle Inlet Angle

ϵ	3.5	3.5	3.5
No. Firings	1	3	3
r*	1.32"	1.32"	1.32"
R^*/r^*	2	2	2
θ_i	5°	15°	30°
θ	15°	15°	15°
Meas. Efficiency	96.0±.5%	95.4±.5%	95.0±.5%
Calc. Efficiency	95.7%	95.4%	95.2%

TABLE V

Comparisons of Calculated and Experimental

Effects of Changes in Nozzle Throat Radii

ϵ	3.5	3.5	24	24
Engine	TPC	FPC	BE-1*	FPC
No. Fired	3	3	2	8
r^*	.47"	1.32"	2.50"	1.32"
R^*/r^*	2	2	2	2
θ_i	27.6°	30°	90°	30°
θ	15°	15°	24°	24°
Meas. Efficiency	93.0±.3%	95.4±.3%	95.5±.3%	94.7±.5%
Calc. Efficiency	93.0%	95.4%	95.3%	94.7%

*Efficiency corrected for rubber liner loss

TABLE VI

Comparison of Calculated and Experimental
Effects of Nozzle Contouring

ϵ	24	24	24
No. Fired	8	8	3
r^*	1.32"	1.32"	1.32"
R^*/r^*	2	2	2
L/r^*	9.02	9.02	9.02
θ_1	30°	30°	30°
Contour	Cone	Rao	Mod. Rao
θ_j	24°	33.6°	45°
θ_e	24°	14.2°	12.4°
Meas. efficiency*	100.0%	99.9%**	98.1%**
Calc. efficiency*	100.0%	100.1%	98.8%**

* Based on cone efficiency

** Particle Impingement on nozzle lip

TABLE VII

Comparison of Calculated and Experimental

Effects of Nozzle Contouring

ϵ	20	20	20	20	20
No. Fired	4	3	3	3	3
r^*	1.32"	1.32"	1.32"	1.32"	1.32"
R^*/r^*	2	2	2	2	2
L/r^*	9.21	9.21	9.21	9.21	9.21
θ_i	30°	30°	30°	30°	30°
Contour	Cone	Arc	Arc	Arc	Arc
θ_j	21.5°	23.5°	25.0°	26.0°	27.0°
θ_e	21.5°	19.5°	18.0°	17.0°	16.0°
Meas. Efficiency*	100.0%	100.4%	100.7%	100.7%	100.2%
Calc. Efficiency*	100.0%	100.3%	100.5%	100.6%	100.3%

*Based on cone efficiency

TABLE VIII

Comparison of One-Dimensional and Two-Dimensional
Calculated Nozzle Efficiencys

ϵ	3.5	20	24	24	24	24
No. Firings	2	3	12	3	2	2
r^*	1.32"	1.32"	1.32"	1.32"	1.32"	1.32"
R^*/r^*	2	2	2	5	5	5
θ_i	30°	30°	30°	30°	30°	30°
θ	25.2°	21.5°	24°	12°	18°	24°
Efficiency - 1D	100.5%	100.8%	100.8%	100.5%	100.7%	100.8%
Efficiency - 2D						

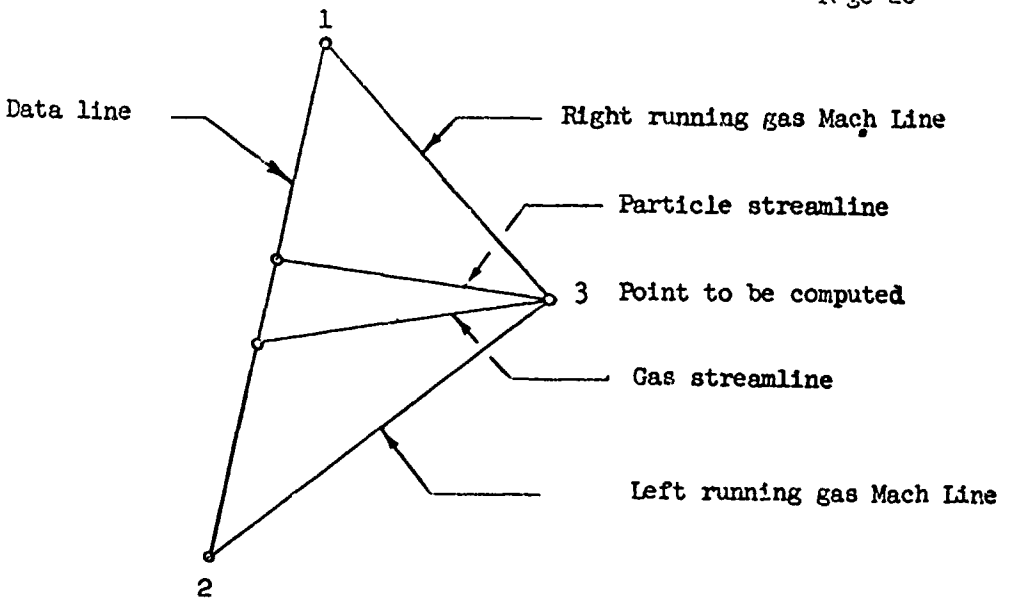

Figure I Gas-Particle Characteristic Mesh

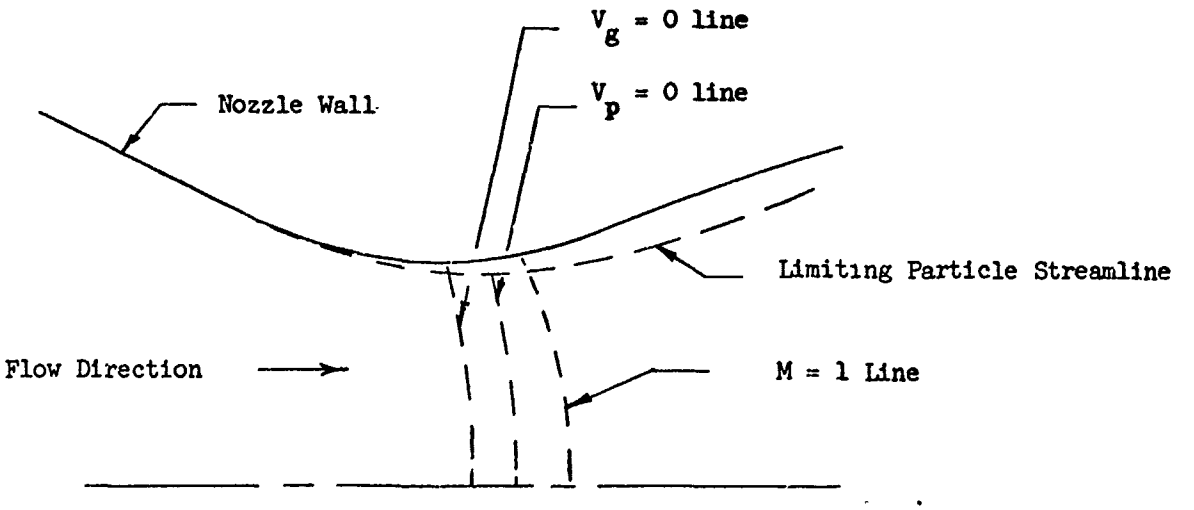

Figure II Gas-Particle Transonic Flow

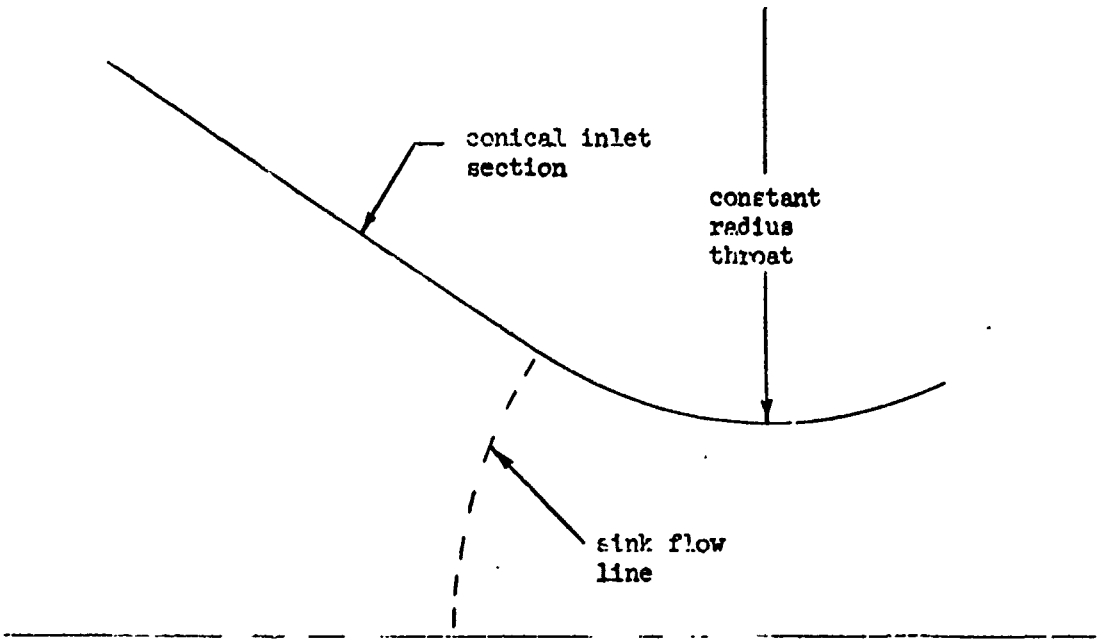

Figure III - Nozzle Inlet and Throat Geometry

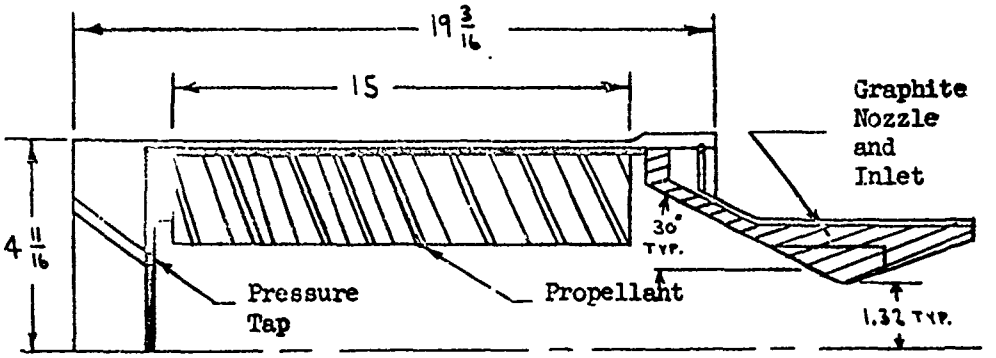

Figure IV Hercules FPC Engine Assembly

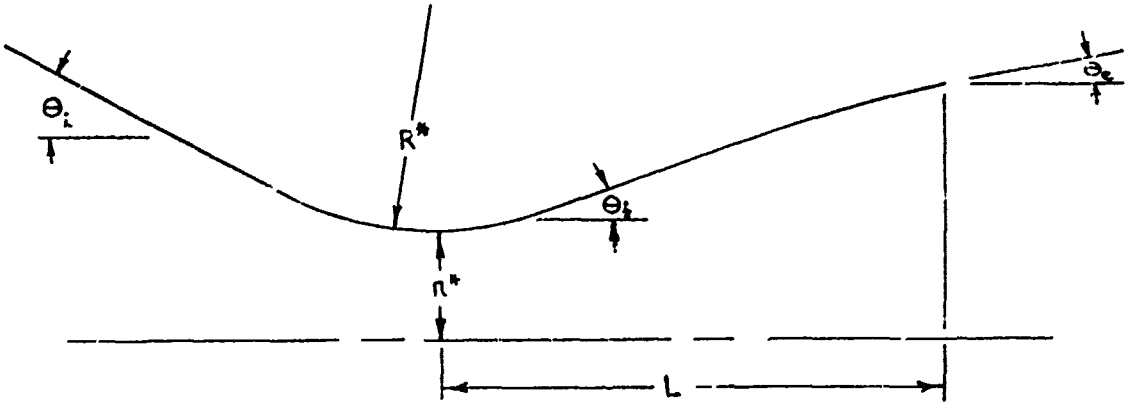

Figure V Nozzle Contour Parameters